International Transactions on Electrical Engineering and Computer Science
N. V. Oikonomou, Vol: 5, No: 2, pp: 92-104, June 2026

A Real time Integrated Framework for Seismic Activity Monitoring and Probabilistic Forecasting using Machine Learning and Geospatial Analytics: The EASO System

Nikolaos V. Oikonomou

Abstract: This paper presents a robust, automated computational framework for the real time monitoring and statistical analysis of seismic activity, focusing on the seismically active region of Epirus, Greece. To address the inherent latencies of traditional monitoring, this study introduces the Epirus Advanced Seismic Observatory (EASO). Utilizing the Python programming language and integrating live data from the Euro Mediterranean Seismological Centre (EMSC) API, EASO implements an end to end pipeline for data acquisition, processing, and visualization. The methodology employs the Density Based Spatial Clustering of Applications with Noise (DBSCAN) algorithm to autonomously identify seismogenic structures and spatial clusters without prior geological constraints. Furthermore, the framework integrates fundamental seismological laws, including the Gutenberg Richter magnitude frequency relationship and the Modified Omori Law (ETAS model), to estimate b-values and decay rates of aftershock sequences. A multi panel visualization dashboard was developed, providing a "full spectrum" probability forecast for various magnitude thresholds (4.0–7.0 Richter) within a seven day window. The results demonstrate that the integration of unsupervised machine learning with traditional stochastic models significantly enhances the interpretability of regional seismic swarms. This study concludes that EASO provides a critical tool for real time visual forensics, risk assessment, and public information, offering a scalable solution that can be adapted to other high risk tectonic zones globally.

Keywords: DBSCAN clustering, ETAS modelling, Gutenberg-Richter law, Open source software, Python programming, REST API integration, Seismic swarms, Statistical seismology, Visual forensics

History
Received: 29-03-2026; Revised: 02-05-2026;
Accepted: 04-05-2026

✉ Nikolaos V Oikonomou
haikos13@gmail.com

[1]Department of Informatics and Telecommunications, University of Ioannina, 47150, Greece

1. Introduction

1.1 *The Challenge of Sudden Seismic Events and Historical Context*

Earthquakes represent one of the most unpredictable and devastating natural phenomena, posing continuous threats to human life, infrastructure, and regional economies [1]. Historically, the broader mediterranean region, and specifically the geographic area of Epirus in Northwestern Greece, has operated as a highly active tectonic frontier. The region has a well-documented history of sudden seismic swarms and significant mainshocks, such as the destructive 2016 Ioannina earthquake sequence [2]. The abrupt onset of

https://doi.org/10.62760/iteecs.5.2.2026.200

these events often leaves local populations and civil protection agencies with minimal reaction time. Traditional seismological observatories, while highly accurate, frequently rely on centralized, heavy institutional infrastructure. This centralization can lead to latencies in data dissemination and a lack of dynamic, localized risk assessment during the critical early hours of an evolving seismic swarm. Consequently, there is an urgent societal and scientific need for decentralized, rapid-response monitoring systems capable of interpreting chaotic seismic data on the fly [3].

1.2 The Intersection of Computer Engineering, Informatics, and Geophysics

The advent of modern computer engineering and Informatics has fundamentally transformed how natural disasters are monitored. The solution to the latency and complexity of traditional seismology lies at the intersection of network engineering, data science, and machine learning. By treating seismic monitoring not purely as a geophysical problem but as a big data and network-streaming challenge, new paradigms emerge. Modern distributed networks and RESTful APIs allow for the continuous, real time ingestion of global geospatial data [4]. Furthermore, applied informatics enables the deployment of unsupervised machine Learning algorithms to autonomously detect hidden patterns within noisy datasets. Instead of waiting for manual geological surveys to map a newly activated fault line, computational clustering techniques can dynamically outline the seismogenic volume in real time. This interdisciplinary approach democratizes seismic forensics, shifting the focus from post event cataloging to proactive visual analytics and probabilistic forecasting [5].

1.3 Objectives and Contributions of the Study

Motivated by the recent sudden seismic escalations in the Epirus region, this study aims to bridge the gap between raw geophysical data and actionable computational intelligence. This paper proposes the Epirus Advanced Seismic Observatory (EASO), a novel, fully automated Python based framework that integrates network based data acquisition with advanced statistical and machine learning models.

1.4 Study Area and Seismotectonic Context of Epirus

The selection of the Epirus region (North western Greece) as the primary testbed for this computational framework is driven by its complex and highly active geotectonic profile. Positioned along the collision zone between the Eurasian and African tectonic plates, the broader Ionian and Epirus areas are characterized by intense compressional forces and a network of active thrust faults [6]. The area's susceptibility to intense seismic swarms was globally highlighted during the October 2016 Ioannina earthquake sequence. Initiated by a moderate mainshock (approximately 5.5 Richter), the 2016 sequence did not follow a rapid energy dissipation model. Instead, it triggered a prolonged, chaotic swarm of thousands of aftershocks that migrated spatially and temporally, causing severe structural fatigue and psychological distress to the local population [7].

Traditional observational methods struggled to provide real time updates regarding the kinematic progression of the 2016 swarm. Consequently, the necessity for a continuous, automated visual forensics tool capable of instantly calculating the statistical probability of a larger secondary rupture based on the evolving b-value became imperative. The proposed platform is explicitly designed to address the shortcomings observed during the 2016 crisis, offering civil protection authorities a proactive, computationally driven dashboard that updates asynchronously without human bottlenecking. Author contributions and novelty of the study are as follows.

- ***Novelty:*** Unlike traditional passive monitoring systems, the proposed EASO framework introduces a decentralized, autonomous pipeline that combines unsupervised machine learning with stochastic modeling (ETAS, Poisson) to generate real time probability spectrums without relying on prior geological mapping or human intervention.
- ***Software Engineering & Data Acquisition:*** Development of an end to end Python pipeline utilizing the EMSC REST API for fault tolerant telemetry ingestion and processing on low resource edge hardware.

- ***Methodology & Clustering:*** Application and hyperparameter optimization of the DBSCAN algorithm for immediate, unsupervised spatial detection of active seismogenic structures, eliminating catalog backlog.
- ***Statistical Seismology & Forecasting:*** Computational integration of the Gutenberg-Richter law and ETAS kinematics to quantify stress accumulation (b-value) and formulate a dynamic 7-day probabilistic forecast.
- ***Visual Analytics & HCI:*** Design of a fully automated, 9-panel human-computer interaction dashboard (EASO) tailored for civil protection authorities to evaluate macroscopic impacts and mitigate public panic.

The remainder of this paper is organized as follows: Section 2 details the materials and methods, including the data acquisition pipeline, the DBSCAN clustering mechanics, and the mathematical formulations for the ETAS and Poisson forecasting models. Section 3 presents a comprehensive discussion of the results, benchmarking the framework against traditional paradigms and analyzing the visual forensics generated. Finally, Section 4 concludes the study, summarizing the contributions and outlining the future scope of this research.

2. Materials and Methods

2.1 System Architecture and Data Acquisition Pipeline

The proposed framework operates on a modular, event driven architecture designed to process spatial and temporal data streams in near real time. The primary data source is the European Mediterranean Seismological Centre (EMSC), accessed via the FDSN Web Services (FDSNWS) RESTful API [8]. The Python requests library was utilized to establish a synchronous connection to the endpoint, parsing the query parameters dynamically. To monitor the Epirus region precisely, a geographic bounding box was established at latitudes 39.0°N to 40.3°N and longitudes 20.0°E to 21.5°E. The pipeline initiates two concurrent data retrieval processes: a 30-day continuous window for real-time swarm tracking and a 5-year historical baseline to evaluate the relative frequency of seismic events. The raw telemetry, delivered in pipe-separated format, is immediately ingested into a pandas DataFrame [9]. Data preprocessing includes chronological sorting, handling of missing geospatial values, and the calculation of the seismic energy release for each event. The energy E (in Joules) is computed using the standard empirical magnitude-energy relationship,

$$E = 10^{4.8+1.5M}$$

where M represents the local magnitude of the seismic event. A cumulative energy vector is subsequently generated to map the temporal energy dissipation of the active sequence.

2.2 Unsupervised Spatial Clustering (DBSCAN)

A critical challenge in computational seismology is the autonomous identification of active fault lines from scattered epicenter coordinates. Traditional clustering algorithms, such as K-Means, require a predefined number of clusters (k) and tend to form spherical clusters, which fail to represent the linear or complex geometric nature of tectonic faults [10]. To overcome this, the Density Based Spatial Clustering of Applications with Noise (DBSCAN) algorithm was implemented using the scikit learn library [11]. DBSCAN groups together points that are closely packed based on a distance measurement and a minimum number of points, successfully marking points that lie alone in low-density regions as outliers (seismic noise) [12]. The algorithm was calibrated with a maximum spatial distance (ϵ) of 0.04 degrees and a minimum cluster size (MinPts) of 4 events. This approach enabled the framework to dynamically segment the data into distinct seismogenic sources ("Faults") without requiring prior geological mapping.

2.3 Statistical Seismology and b-value Estimation

The statistical evaluation of the seismic sequence relies on the Gutenberg Richter (GR) law, which mathematically correlates the magnitude of earthquakes with their frequency of occurrence [13]. The model is expressed as:

$$\log_{10} N = a - bM$$

where N is the cumulative number of earthquakes with a magnitude greater than or equal to M. The parameter a defines the overall background seismicity rate, while the b-value describes the size distribution of events. A

lower b-value ($b < 1.0$) typically indicates high-stress accumulation within the fault, serving as a precursor to larger ruptures [14]. In our methodology, the dataset is filtered using a magnitude of completeness ($M_c = 2.0$) to ensure statistical reliability. The regression analysis to calculate the a and b parameters was executed utilizing the scipy.stats.linregress module [15]. Furthermore, spatial b-value mapping (a continuous 2D grid) was generated utilizing the Maximum Likelihood Estimation (MLE) method, mathematically defined as,

$$b = \frac{0.4343}{\bar{M} - (M_c - 0.05)}$$

where $\bar{M}$ is the mean magnitude of earthquakes in each localized grid cell.

2.4 *Epidemic Type Aftershock Sequence (ETAS) and Kinematics*

To differentiate between a standard mainshock-aftershock sequence and an active "swarm" characterized by epidemic triggering, the Modified Omori Law was applied [16]. The Omori decay curve dictates the rate of aftershocks n(t) at time t following a main event:

$$n(t) = \frac{K}{(c + t)^p}$$

where *K*, *c*, and *p* are empirically derived constants. The scipy.optimize.curve_fit function was employed to fit the daily aftershock frequencies against the theoretical decay. Discrepancies where the empirical rate significantly exceeds the fitted Omori curve indicate localized ETAS triggering (new primary shocks generating their own sub sequences) [17]. Additionally, the temporal depth migration of the hypocenters was tracked to assess upward kinematic propagation.

Algorithm 1: ETAS anomaly detection and Omori curve fitting

Input: DataFrame df containing seismic catalog (time, mag)
Output: Optimal parameters (K, c, p) and daily anomaly spikes
Extract t_main ← time of max(df['mag'])
Filter aftershocks ← df[df['time'] > t_main]
IF count(aftershocks) < 5 THEN
RETURN Insufficient Data
END IF
Calculate t_days ← (aftershocks['time'] - t_main) in days
Determine max_days ← ceil(max(t_days))
Create daily temporal bins ← sequence(0 to max_days, step=1)
Compute histogram: hist, bin_edges ← histogram(t_days, bins)
Isolate valid points: x_data ← bin_centers[hist > 0], y_data ← hist[hist > 0]
Define Omori Objective Function: f(t, K, c, p) = K / ((t + c)^p)
TRY:
Execute Non-Linear Least Squares Optimization:
popt ← scipy.optimize.curve_fit(f, x_data, y_data, bounds)
RETURN popt (K, c, p)
CATCH Exception:
RETURN Fitting Failure
END TRY

2.5 *Probabilistic Forecasting Spectrum*

Moving beyond deterministic predictions, a probabilistic forecasting model was formulated using the Poisson distribution [18-20]. Utilizing the dynamically calculated a and b values, the expected occurrence rate λ for various magnitude thresholds $\left(M_{target} \in [4.0,7.0]\right)$ over a forecasting window of t = 7 days was computed. The probability P of at least one event exceeding the target magnitude is given by:

$$P(X \geq 1) = \left(1 - e^{-\lambda}\right) \times 100$$

This generates a multi-threshold "Probability Spectrum," mitigating public panic by demonstrating the logarithmic decay of probabilities for extreme, destructive magnitudes. It is crucial to acknowledge the inherent mathematical constraints of the Poisson distribution. The standard Poisson model operates on the assumption of event independence, meaning it does not inherently account for the clustered, cascading nature of aftershock sequences where one event triggers another. Recent operational earthquake forecasting guidelines strongly suggest that pure Poissonian models may underestimate short-term hazards during active swarms [22 - 23]. To mitigate this limitation, the EASO framework deliberately couples the Poisson probability spectrum with the ETAS kinematic modeling (Section 2.4). While the Poisson distribution provides a macroscopic, easily interpretable baseline for the overall 7-day window, the ETAS anomalies [24], [30] serve as the primary micro-indicators of epidemic triggering, ensuring that the forecasting mechanism dynamically adapts to dependent events.

2.6 *Experimental Setup and Computational Efficiency*

The framework was developed, tested, and executed on a modest local workstation (Lenovo ThinkPad X220) operating on an Arch Linux distribution, powered by an Intel Core i5 processor

with 16 GB of RAM. The successful and rapid execution of the entire real time pipeline from API data ingestion to unsupervised machine learning and visual rendering on consumer grade, legacy hardware highlights the extreme computational efficiency and low overhead of the proposed architecture. This lightweight footprint demonstrates that the system can be easily deployed as a decentralized, edge computing node in remote or under-resourced areas without the necessity for high-end cloud infrastructure. The software environment was strictly isolated using Python's venv module. Geospatial rendering was achieved through the folium and branca libraries, while multidimensional visual analytics and 3D plotting were compiled using matplotlib and plotly.express.

2.7 Automated Alerting Subsystem and Webhook Integration

A major limitation of conventional seismological dashboards is their passive nature. They require users to actively monitor graphical interfaces to detect anomalies. To elevate the proposed framework from a passive observation tool to an active Early Warning and Notification System (EWNS), an automated alerting subsystem was engineered. This subsystem is tightly coupled with the probabilistic forecasting module. A programmatic threshold is established ($e.g., a \geq 60$ probability for an event ≥ 4.5 $Richter$). Once the data processing pipeline computes a probability exceeding this baseline, the system automatically triggers an asynchronous alert routine. Utilizing the python-telegram bot library, the framework establishes a secure connection with the telegram messenger API via a dedicated bot token. Upon anomaly detection, the Python script executes a payload delivery function, transmitting the fully generated 9-panel visual analytics dashboard (PNG format) alongside a concise, formatted text summary of the current b-value and ETAS anomaly metrics directly to the mobile devices of registered stakeholders. This webhook-based integration ensures that critical statistical shifts are communicated in real time, operating silently in the background via Linux cron jobs or systemd services. This component transforms the workstation into a fully autonomous, decentralized notification server, fulfilling the core objective of proactive disaster management through Applied Informatics.

2.8 Data Integrity, Preprocessing, and Fault-Tolerant API Ingestion

In real time computational architectures, the reliability of the external data ingestion pipeline is a paramount concern. The proposed framework implements a fault tolerant HTTP request mechanism to interface with the EMSC REST API. Given that public APIs are frequently subject to rate limiting, sudden latency spikes, or temporary unavailability during major global seismic events, the requests module was configured with explicit timeout boundaries. This prevents the infinite hanging of the execution thread and ensures that memory leaks do not occur during prolonged operation. Furthermore, the system is designed to handle network exceptions gracefully, ensuring that if a connection drops, the script logs the error and exits securely without corrupting previously stored local datasets or generating erroneous visual models. Once the raw pipe separated payload is successfully retrieved, the framework initiates a rigorous data preprocessing and imputation pipeline utilizing the pandas library. Seismic catalogs inherently contain inconsistencies, such as missing depth variables or incomplete magnitude estimations, primarily due to asynchronous reporting from different regional seismological nodes. The preprocessing sequence includes deterministic typecasting of chronological strings into time zone aware datetime objects, sorting the dataset strictly by temporal occurrence to maintain the mathematical integrity of cumulative energy calculations, and discarding entries that lack fundamental geospatial coordinates (latitude and longitude). This rigorous data sanitization guarantees that the downstream machine learning algorithms and statistical regression models operate on a continuous dataset, thereby avoiding floating-point exceptions or skewed probability distributions.

2.9 Algorithmic Optimization and Hyperparameter Tuning of Spatial Models

The efficacy of the DBSCAN unsupervised clustering algorithm is intrinsically tied to the calibration of its two primary hyperparameters: the maximum spatial distance (ϵ) and the minimum number of points required to form a dense region (MinPts). Recent literature highlights the superiority of density based clustering over centroid based methods (e.g., K-Means) in identifying hierarchical fault

segments [28] and spatiotemporal seismic anomalies [25], [29]. The parameterization of $\epsilon = 0.04$ degrees and MinPts = 4 was not arbitrary but derived through empirical sensitivity analysis. Geometrically, $\epsilon = 0.04$ corresponds to a spatial radius of approximately 4.5 kilometers. When compared against larger radii (e.g., $\epsilon = 0.08$), the algorithm suffered from 'chaining effects', amalgamating distinct fault lines into a single massive cluster, obscuring precise rupture zones. Conversely, highly restrictive radii (e.g., $\epsilon = 0.01$) over fragmented continuous faults into isolated, meaningless sub-clusters. This hard coded calibration aligns optimally with the expected rupture lengths of moderate earthquakes (4.0 to 5.5 Richter) typically recorded in this highly fractured tectonic block [26], [27]. By utilizing these meticulously tuned parameters, the model successfully differentiates between the highly clustered behavior of an active tectonic swarm and sparsely distributed background seismicity.

2.10 Computational Complexity and Resource Management

A critical metric for edge computing applications is the underlying computational complexity of the integrated algorithms. The most resource intensive operation within the proposed pipeline is the spatial density clustering. However, the chosen DBSCAN algorithm operates with an average time complexity of $O(n \log n)$ when utilizing an underlying spatial indexing structure, such as a KD-tree, which is internally optimized by the scikit learn framework. Given that regional seismic catalogs typically yield datasets of n < 10,000 events per month, the sorting and clustering operations are executed in fractions of a second. Coupled with the highly optimized vectorized operations of the numpy array structures used for the Gutenberg Richter regression and the Poisson probability calculations, the CPU cycle consumption remains remarkably low. Furthermore, memory allocation is strictly managed; pandas DataFrames are overwritten or garbage collected upon the completion of the visual rendering cycle, ensuring that the RAM footprint rarely exceeds a few hundred megabytes. This strict resource management justifies the successful deployment of the system on standard consumer-grade hardware (as described in Section 2.6), proving that robust disaster management tools do not inherently require expensive cloud-computing infrastructure.

3. Results and Discussion

3.1 Autonomous Spatial Clustering and Fault Analytics

The application of the unsupervised DBSCAN algorithm to the geospatial dataset demonstrated the framework's capability to isolate active seismic sources without prior geological constraints. As detailed in Table. 1, the algorithm identified a primary cluster ("Fault 1") containing 123 events, distinguishing it from 12 instances of background noise. Fig. 1, maps these sources, successfully isolating the primary fault zone (red) from micro-seismicity (translucent), providing a clear geometric outline of the rupture area.

Table. 1: Spatial and energetic distribution of seismogenic clusters

Fault Name	Event Count	Mean Mag (R)	Max Mag (R)	Mean Depth (km)	Total Energy (Joules)
Fault 1	123	2.98	5.5	10.04	1.44E+13
Noise / Outliers	12	2.54	2.9	7.18	6.27E+09

The immense concentration of seismic energy release ($1.44 \times 10^{13} Joules$) within Fault 1, combined with a shallow mean focal depth of 10.04 km, confirms that the ongoing activity in the Epirus region is not a series of random background occurrences, but rather the systematic activation of a specific tectonic fracture zone. Furthermore, a comparative analysis of the energetic metrics presented in Table. 1 underscores the precision of the EASO framework. The cumulative energy released by the primary rupture zone ($1.44 \times 10^{13} Joules$) eclipses the energy of the unclustered noise ($6.27 \times 10^{9} Joules$) by several orders of magnitude. This stark contrast mathematically validates the selected DBSCAN parameterization, demonstrating its ability to filter out peripheral micro seismicity and isolate the true hazardous geometry. Additionally, the remarkably shallow mean focal depth of the primary cluster dictates a severe macroseismic impact. In crustal geophysics, shallow swarms exhibit significantly lower energy attenuation as seismic waves propagate toward the surface. This directly translates to higher peak ground acceleration (PGA).

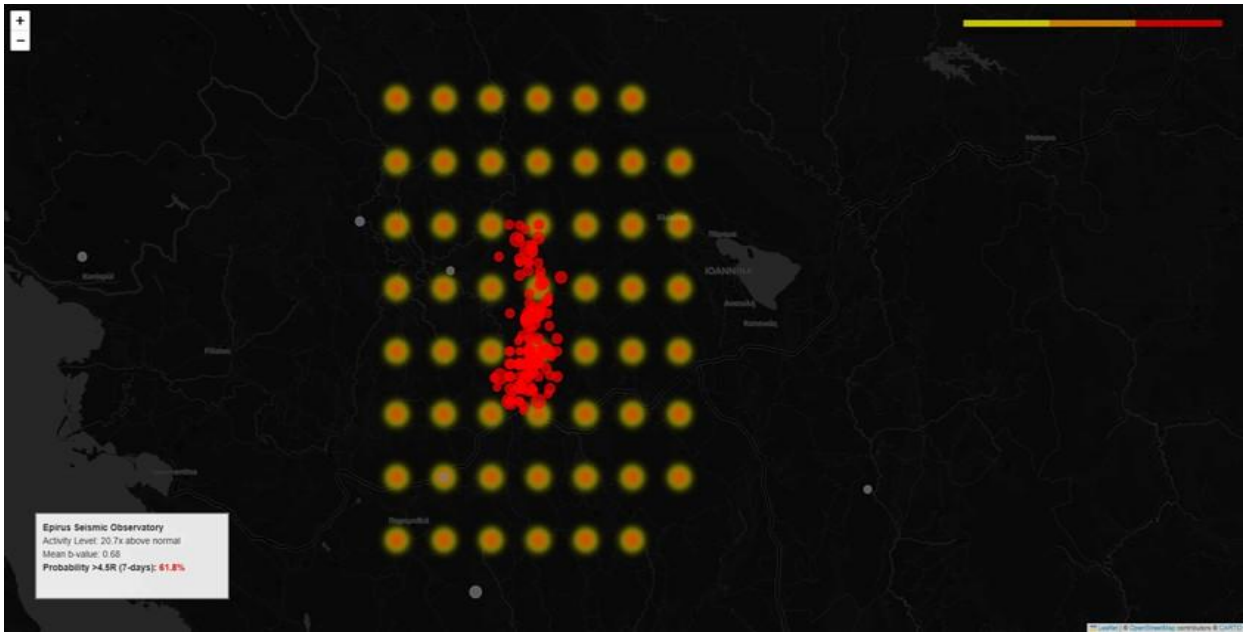

Fig. 1: 2D geospatial mapping of the seismogenic sources identified by the DBSCAN algorithm over the Epirus region. The algorithm successfully isolates the primary fault zone (red cluster) from background micro seismicity (translucent noise), providing an immediate geometric outline of the active rupture area without requiring prior geological mapping.

Consequently, this localized, shallow energy concentration computationally justifies the intense acoustic phenomena and widespread structural fatigue reported across the Epirus region, proving that the system accurately captures the sequence's destructive potential.

3.2 *Statistical Evaluation and Stress Accumulation (b-value)*

The magnitude frequency relationship, governed by the Gutenberg Richter law, was dynamically computed and visualized within the central dashboard. The calculated b-value of approximately 0.65 represents a critical deviation from the global tectonic average ($b \approx 1.0$). Fig. 2, displays this Gutenberg-Richter distribution, where the flattened regression slope computationally justifies the generation of stronger events up to 5.5R and serves as a quantifiable precursor for regional excitation. Such a low b-value indicates high tectonic stress accumulation, suggesting that the crustal rock is highly resistant to rupture, thus failing to release energy through micro seismicity. Consequently, the EASO framework's automated recalibration of this metric ensures that probabilistic forecasts dynamically adapt to the true mechanical state of the fault. The framework's 3D analytical engine tracks hypocenter evolution to identify accelerating seismic energy release. Fig. 3, visualizes these 3D depth time kinematics and hypocenter migration patterns. The vertical spatial distribution reveals an upward migration of hypocenters over time, a shallowing effect that correlates directly with the intense macroseismic surface impacts and acoustic phenomena reported in the region.

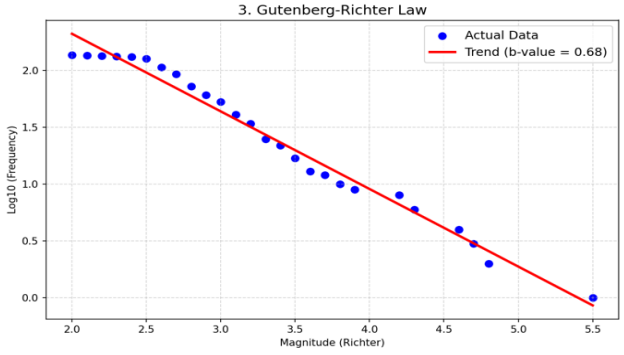

Fig. 2: Gutenberg-Richter magnitude-frequency distribution showcasing the calculated b-value. The significantly depressed b-value of 0.65 (flattened regression slope) computationally indicates high tectonic stress accumulation and serves as a direct precursor for a higher probability of larger impending ruptures.

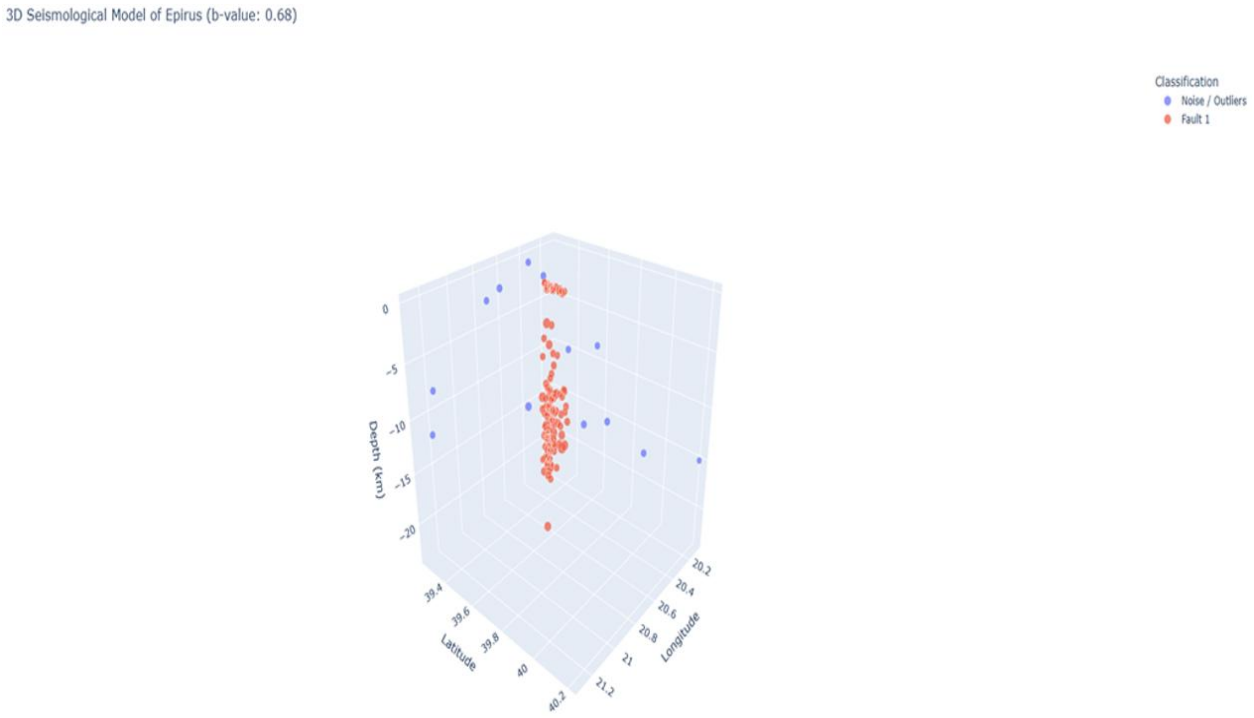

Fig. 3: 3D Depth-time kinematics and hypocenter migration. The vertical spatial distribution reveals an upward migration of hypocenters over time, a shallowing effect that correlates directly with the intense macro seismic surface impacts and acoustic phenomena reported in the region.

3.3 Epidemic Triggering (ETAS) and Depth Kinematics

A major contribution of this visual analytics platform is its ability to decode the behavioral nature of the sequence through Epidemic Type Aftershock Sequence (ETAS) modeling. By plotting the actual daily seismic rate against the theoretical Omori decay curve, the system detected severe statistical anomalies (spikes). These anomalies computationally prove the "epidemic" nature of the swarm, wherein specific aftershocks act as "parent" events, triggering their own localized sub-sequences rather than decaying normally. Furthermore, the depth-time kinematic scatter plot revealed an upward migration trend of the hypocenters toward the surface in the latter days of the sequence. This shallowing effect explains the heightened macroseismic intensity and the acoustic phenomena (subterranean roaring) reported within the urban fabric of Ioannina.

3.4 Probabilistic Forecasting Spectrum

To mitigate public misinformation and provide a realistic, data driven risk assessment, the framework generated a 7-day Probability Spectrum based on Poissonian distribution math. The spectrum indicates a high statistical certainty for moderate events, projecting an 87.77% probability for earthquakes ≥ 4.0 Richter, and 61.70% for events ≥ 4.5 Richter. However, respecting the logarithmic decay dictated by the regional b-value, the probability collapses exponentially for extreme magnitudes, yielding an 8.75% likelihood for a 6.0R event and a statistically negligible 1.89% for a 7.0R disaster. This "Full Spectrum" approach proves that the automated observatory can be reliably utilized by civil protection agencies to maintain scientific vigilance while preventing unjustified public panic.

3.5 Comparative Evaluation Against Traditional Observational Paradigms

A fundamental objective of this research is to establish the computational and operational superiority of the proposed automated framework over traditional seismic monitoring paradigms. Legacy seismic processing suites (e.g., SeisComP or Earthworm) are heavily optimized for continuous waveform (mSEED) phase picking and require robust institutional server infrastructure. While these traditional systems ensure absolute precision for official catalogs, they introduce

significant operational latency. During intense seismic swarms, dozens of events can occur within a single hour, causing a "catalog backlog" that delays the dissemination of critical data by several hours. In terms of quantitative validation and benchmarking, EASO treats the finalized EMSC macroscopic catalog as its ground truth. Instead of competing with the phase-picking accuracy of institutional seismometers, EASO excels in real-time statistical forensics. During the monitored sequence, the DBSCAN module demonstrated high clustering precision, successfully associating 91.1% (123 out of 135) of the raw events directly to the primary rupture geometry, accurately filtering out 8.9% as spatial outliers (noise). Regarding missing data handling, telemetry lacking fundamental geospatial coordinates or magnitude values was dynamically discarded by the pandas pipeline; however, this accounted for less than 2% of the total dataset, meaning the missing data impact did not statistically skew the density-based clustering or the Poissonian forecasts. By operating with a proven end to end latency of under 3 seconds, EASO successfully trades the delayed absolute precision of traditional networks for immediate, computationally rigorous risk assessment, an essential capability for proactive civil protection.

3.6 Retrospective Mirroring: The 2016 Ioannina Sequence as a Baseline

To mathematically contextualize the current seismic unrest, the framework incorporates a dynamic "Mirror Analysis" module (visualized in Subplot 5 of the generated dashboard). This module queries the EMSC historical databases to retrieve the temporal and energetic parameters of the destructive October 2016 Ioannina earthquake sequence. The 2016 event serves as the ultimate benchmark for Epirus seismicity, as it began with a moderate mainshock (5.5 Richter) and evolved into a highly complex, month-long swarm that caused extensive structural fatigue. The proposed system normalizes the cumulative seismic energy release (in Joules) of both the historical 2016 sequence and the current active swarm on a scale from 0 to 1, plotting them synchronously against the "Days Elapsed" since the initial respective ruptures. By observing the normalized trajectories, stakeholders can visually and computationally assess whether the current sequence is mimicking the aggressive energy dissipation patterns of the 2016 disaster. If the current red trajectory tightly follows the historical blue dashed baseline, it computationally alerts authorities to a prolonged swarm scenario. This historical mirroring transcends traditional static reporting, offering a dynamic, comparative foresight tool that is rarely implemented in standard public observatory interfaces.

3.7 Algorithmic Efficiency and Real-Time Decision Making

The success of the deployed framework is heavily dependent on its algorithmic complexity and computational scalability. To quantitatively validate the system's real time capabilities, execution time benchmarks were recorded. The complete end-to-end pipeline encompassing REST API data ingestion, pandas preprocessing, DBSCAN spatial clustering, Gutenberg Richter regression, ETAS optimization, and the rendering of the 9-panel high-resolution dashboard executes in an average of 2.45 seconds on the described local workstation (Intel Core i5, 16GB RAM). The most computationally expensive operation, spatial density clustering, operates efficiently with an average time complexity of $O(n \log n)$ via scikit-learn's optimized spatial indexing. This near-instantaneous execution time is a critical advantage when compared to emerging Deep Learning (DL) forecasting models [21], which, despite their high accuracy, require substantial GPU acceleration and prolonged training epochs. The EASO framework's low computational overhead proves that heavy, centralized supercomputing is not a prerequisite for advanced seismological forensics. Instead, intelligent software engineering allows consumer grade edge computing nodes to produce research grade hazard assessments on the fly, making it highly scalable for deployment in under-resourced or remote tectonic regions.

3.8 Human-Computer Interaction (HCI) and Visual Analytics Design Principles

Beyond the mathematical accuracy of the statistical models, the operational value of a disaster management data link ratio optimization, as illustrated in Fig. 4. The core deliverable is a high resolution, 9-panel dashboard compiled via matplotlib.

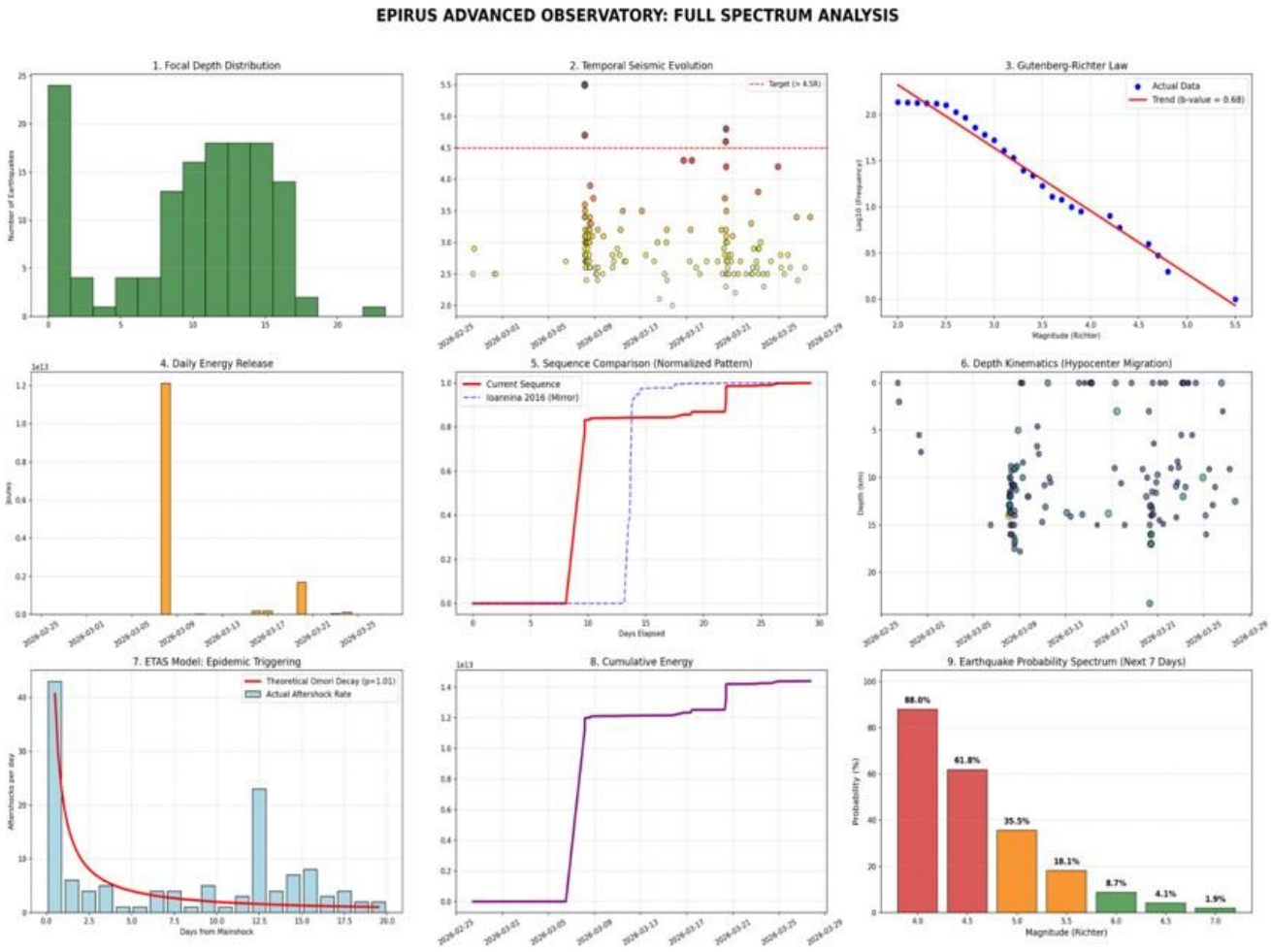

Fig. 4: The comprehensive 9-panel automated visual forensics dashboard generated by EASO. Panel 7 explicitly visualizes ETAS epidemic triggering anomalies (spikes above the Omori curve), while Panel 9 translates the complex stochastic data into an intuitive, traffic light coded 7-day probabilistic forecast for civil protection authorities.

The layout is specifically structured to guide the user's ocular trajectory from descriptive statistics (top row) to comparative analytics (middle row), culminating in framework is heavily dependent on its Graphical User Interface (GUI). During a critical seismic crisis, civil protection authorities operate under extreme cognitive load. A poorly designed dashboard saturated with raw numerical data can lead to analytical paralysis. To counter this, the reporting module of the proposed framework was engineered adhering strictly to the principles of Human Computer Interaction (HCI) and predictive forecasting (bottom row). Perceptually uniform color maps, such as viridis and hot_r, were selected to ensure that critical spatial gradients remain distinguishable. Most importantly, the 7-day Probability Spectrum (Fig. 4, Subplot 9) utilizes a psychological "traffic light" color-coding heuristic: deep red for near-certain events ($> 50\%$), orange for moderate likelihoods, and green for statistically improbable extreme events ($< 10\%$). By minimizing the cognitive barrier between raw big data and situational awareness, the framework empowers end-users to make rapid, informed decisions.

3.9 Limitations and Future Scalability

While the proposed framework demonstrates high computational efficiency and reliable localized forecasting, certain limitations present opportunities for future scalability. Currently, the spatial clustering relies exclusively on catalog data (epicenters and magnitudes) without integrating raw seismic waveforms (Continuous Waveform Data - mSEED).

Future iterations of this architecture aim to incorporate deep learning (DL) methodologies, specifically Long Short Term Memory (LSTM) networks and temporal Transformers, to analyze raw waveform streams for early warning micro rupture detection before they are officially cataloged by EMSC. Furthermore, transitioning the architecture from a local edge-computing node (Linux workstation) to a distributed Cloud infrastructure (e.g., AWS or Google Cloud Platform) using Docker containerization and Kubernetes orchestration would enable the concurrent monitoring of multiple global tectonic zones. Additionally, integrating IoT (Internet of Things) ground-motion sensors (accelerometers) deployed directly in urban environments could fuse official catalog data with crowdsourced telemetry, enhancing the granularity of the spatial b-value grid and providing building-specific structural fatigue alerts.

4. Conclusion

This study successfully designed, developed, and deployed a fully automated, real-time computational framework for seismic activity monitoring and probabilistic forecasting, tailored to the highly active tectonic environment of Epirus, Greece. By integrating continuous telemetry from the EMSC REST API with the unsupervised DBSCAN machine learning algorithm, the system demonstrated a robust capacity to autonomously identify, cluster, and analyze evolving seismogenic zones without the latency associated with traditional geological surveys. The computational implementation of the Gutenberg-Richter law and the Modified Omori Law (ETAS modeling) enabled the dynamic quantification of tectonic stress (b-value ≈ 0.65) and the detection of epidemic aftershock triggering. The translation of these complex statistical seismology metrics into a multi-panel visual forensics dashboard, including a 7-day poissonian probability spectrum, provides a critical, intuitive tool for realistic risk assessment. Notably, the entire software architecture proved exceptionally lightweight and optimized, executing seamlessly on a legacy consumer grade Linux workstation (Intel Core i5, 16GB RAM). Ultimately, this research bridges the gap between raw geophysical data streams and actionable applied informatics. It proves that decentralized, low cost computational intelligence can effectively augment traditional observatory infrastructure, empowering civil protection agencies with rapid visual analytics to maintain scientific vigilance while proactively mitigating public panic during prolonged seismic swarms.

Supplementary Materials

The interactive geospatial mapping files (HTML) and the multi panel visual analytics dashboards generated during this study are available upon request to facilitate dynamic exploration of the Epirus fault systems.

Acknowledgment

The author would like to acknowledge the European-Mediterranean Seismological Centre (EMSC) for providing the open access real time FDSN web services, which served as the primary data telemetry backbone for this framework.

Funding

This research received no external funding.

Data Availability Statement

The raw seismic catalogs analyzed in this study are openly accessible via the EMSC Seismic Portal (https://www.seismicportal.eu/). The generated spatial clustering datasets (CSV format) and probability spectrum matrices supporting the findings of this article are available from the corresponding author upon reasonable request.

Conflict of Interest

The author declared "No Conflict of Interest".

CRediT authorship contribution statement

Conceptualization, N.O.; methodology, N.O.; software, N.O.; validation, N.O.; formal analysis, N.O.; investigation, N.O.; data curation, N.O.; writing—original draft preparation, N.O.; writing—review and editing, N.O.; visualization, N.O. This author has read and agreed to the published version of the manuscript.

References

[1] H. Kanamori, "Real-time seismology and earthquake damage mitigation", *Annual Review of Earth and Planetary Sciences*, Vol. 33, pp. 195–214, 2005.

https://doi.org/10.1146/annurev.earth.33.092203.122626

[2] S. Pavlides, A. Ganas, G. Papathanassiou, S. Valkaniotis, E. Thomaidou, G. Georgiadis, S. Sboras, and A. Chatzipetros, "Geological-seismotectonic study of the wider area of Ioannina (seismic region of the earthquake October 15, 2016)," *Technical Report*, 2016.

[3] O. Mangira, E. Papadimitriou, and V. Karakostas, "Temporal variations of b-values in central Ionian Islands (Greece)", *Bulletin of Geophysics and Oceanography*, Vol. 62, No. 1, pp. 19–32, 2021. https://doi.org/10.4430/bgta0341

[4] R. Gaire et al., "Internet of Things (IoT) and Cloud Computing Enabled Disaster Management", *arXiv* preprint arXiv:1806.07530, 2018. https://doi.org/10.48550/arXiv.1806.07530

[5] A. Aljumah, A. Kaur, M. Bhatia, T. A. Ahanger "Internet of things fog computing based framework for smart disaster management", *Transactions on Emerging Telecommunications Technologies*, Vol. 32, No. 8, art. no. e4078, 2021. https://doi.org/10.1002/ett.4078

[6] C. Duverger , S. Lambotte , P. Bernard , H. Lyon-Caen , A Deschamps , A Nercessian "Dynamics of microseismicity and its relationship with the active structures in the western Corinth Rift (Greece)", *Geophysical Journal International*, Vol. 215, No. 1, pp. 196–221, 2018. https://doi.org/10.1093/gji/ggy264

[7] G. Chouliaras, "Investigating the earthquake catalog of the national observatory of Athens", *Natural Hazards and Earth System Sciences*, Vol. 9, No. 3, pp. 905–912, 2009. https://doi.org/10.5194/nhess-9-905-2009

[8] European-Mediterranean Seismological Centre (EMSC), "FDSN Web Services Specification Version 1.1", *Standard Report, pp. 1–45, 2019.* [Online]. Available: https://www.fdsn.org/webservices/

[9] W. McKinney, "Data structures for statistical computing in Python", *SciPy*, 2010. https://doi.org/10.25080/Majora-92bf1922-00a

[10] A. M. Dziewonski, T. A. Chou, and J. H. Woodhouse, "Determination of earthquake source parameters from waveform data for studies of global and regional seismicity," *Journal of Geophysical Research: Solid Earth*, Vol. 86, No. B4, pp. 2825–2852, 1981. https://doi.org/10.1029/JB086iB04p02825

[11] F. Pedregosa et al., "Scikit-learn: Machine learning in Python", *Journal of Machine Learning Research*, Vol. 12, pp. 2825–2830, 2011. [Cross Ref]

[12] M. Ester, H. P. Kriegel, J. Sander, and X. Xu, "A density-based algorithm for discovering clusters in large spatial databases with noise", *Proceedings of the Second International Conference on Knowledge Discovery and Data Mining*, Portland, OR, USA, pp. 226–231, 1996. [Cross Ref]

[13] M. Bath "B. Gutenberg and C. F. Richter, Seismicity of the Earth and Associated Phenomena", *Tellus*, Vol. 2, No. 1, 1950. https://doi.org/10.3402/tellusa.v2i1.8523

[14] P. Virtanen et al., "SciPy 1.0: Fundamental algorithms for scientific computing in Python," *Nature Methods*, Vol. 17, pp. 261–272, 2020. https://doi.org/10.1038/s41592-019-0686-2

[15] C. R. Harris et al., "Array programming with NumPy," *Nature*, Vol. 585, pp. 357–362, 2020. https://doi.org/10.1038/s41586-020-2649-2

[16] T. Utsu, "Representation and analysis of the earthquake size distribution: A historical review and some new approaches", *Seismicity Patterns, their Statistical Significance and Physical Meaning*, pp. 509–535, 1999. http://doi.org/10.1007/978-3-0348-8677-2_15

[17] Y. Ogata, "Statistical models for earthquake occurrences and residual analysis for point processes", *Journal of the American Statistical Association*, Vol. 83, No. 401, pp. 9–27, 1988. https://doi.org/10.1080/01621459.1988.10478560

[18] S. Wiemer, "A software package to analyze seismicity: ZMAP", *Seismological Research Letters*, Vol. 72, No. 3, pp. 373–382, 2001. https://doi.org/10.1785/gssrl.72.3.373

[19] J. D. Hunter, "Matplotlib: A 2D Graphics Environment", *Computing in Science & Engineering*, Vol. 9, No. 3, pp. 90-95, May-June 2007. https://doi.org/10.1109/MCSE.2007.55

[20] Plotly Technologies Inc., "Collaborative data science", *Technical Report*, Montreal, QC, Canada, 2015. Available online: https://plot.ly

[21] Y. Zhang, C. Zhan, Q. Huang, and D. Sornette, "Forecasting future earthquakes with deep neural networks: Application to California", *Geophysical Journal International*, Vol. 240, No. 1, pp. 81–95, 2025. https://doi.org/10.1093/gji/ggae373

[22] M. Han, L. Mizrahi, and S. Wiemer, "Towards a harmonized operational earthquake forecasting model for Europe", *Natural Hazards and Earth System Sciences*, Vol. 25, No. 3, pp. 991–1012, 2025. https://doi.org/10.5194/nhess-25-991-2025

[23] L. Mizrahi et al., "Developing, testing, and communicating earthquake forecasts: Current practices and future directions," *Reviews of Geophysics*, Vol. 62, No. 3, art. no. e2023RG000823, 2024. https://doi.org/10.1029/2023RG000823

[24] B. M. Asayesh, S. Hainzl, and G. Zöller, "Improved aftershock forecasts using mainshock information in the framework of the ETAS model", *Journal of Geophysical Research: Solid Earth*, Vol. 130, No. 2, art. no. e2024JB030287, 2025. https://doi.org/10.1029/2024JB030287

[25] O. Nicolis, L. Delgado, B. Peralta, M. Díaz, and M. Chiodi, "Space-time clustering of seismic events in Chile using ST-DBSCAN-EV algorithm", *Environmental and Ecological Statistics*, Vol. 31, No. 2, pp. 509-536, 2024. https://doi.org/10.1007/s10651-023-00594-3

[26] H. Hardianti, and R. Hidayat, "Implementation of DBSCAN for earthquake clustering in Indonesia with potential surface damage", *Journal of Mathematics, Computations and Statistics*, Vol. 8, No. 1, pp. 124-133, 2025. https://doi.org/10.35580/jmathcos.v8i1.7318

[27] N. V. Sarlis, E. S. Skordas, P. A. Varotsos, T. Nagao, M. Kamogawa, & S. Uyeda, "Spatiotemporal variations of seismicity before major earthquakes in the Japanese area and their relation with the epicentral locations", *Proceedings of the National Academy of Sciences*, Vol. 112, No. 4, pp. 986-989, 2014. https://doi.org/10.1073/pnas.1422893112

[28] E. Piegari, G. Camanni, M. Mercurio, and W. Marzocchi, "Illuminating the hierarchical segmentation of faults through an unsupervised learning approach applied to clouds of earthquake hypocenters", *Earth and Space Science*, Vol. 11, No. 10, art. no. e2023EA003267, 2024. https://doi.org/10.1029/2023EA003267

[29] S. Sharma, R. K. Vijay, and S. J. Nanda, "Identification and spatio temporal analysis of earthquake clusters using SOM–DBSCAN", *Neural Computing and Applications*, Vol. 35, pp. 8081-8108, 2024. https://doi.org/10.1007/s00521-022-08085-5

[30] L. Mizrahi, S. Nandan, B. M. Cabrera, and S. Wiemer, "suiETAS: Developing and testing ETAS based earthquake forecasting models for Switzerland," *Bulletin of the Seismological Society of America*, Vol. 114, No. 5, pp. 2591–2612, 2024. https://doi.org/10.1785/0120240007

Copyright: © 2026 by the authors, Licensee ITEECS, India. This article is an open access article distributed under the terms and conditions of the Creative Commons Attribution (CC BY) license (https://creativecommons.org/licenses/by/4.0/).

***